

Transverse-field muon spin relaxation investigations of the magnetic penetration depth in the carbide superconductors $Y_2C_2(Br,I)_2$ and YC_2

R. W. Henn, C. Bernhard, R. K. Kremer, Th. Gulden, and A. Simon

Max-Planck-Institut für Festkörperforschung, Heisenbergstraße 1, D-70569 Stuttgart, Germany

Th. Blasius and Ch. Niedermayer

Universität Konstanz, Fakultät für Physik, D-78434 Konstanz, Germany

(Received 9 May 2000)

We present measurements of the temperature and magnetic field ($B_{\text{ext}} < 0.2$ T) dependences of the transverse-field muon spin relaxation rate taken on polycrystalline samples of the layered superconductors $Y_2C_2X_2$, $X = \text{Br, I}$, and the binary carbide YC_2 . The aim of these investigations was to determine the magnetic penetration depth $\lambda(T)$ which is a fundamental parameter of the superconducting state. The magnetic-field dependence of the muon-depolarization rate below T_c is discussed. An analysis of the temperature dependence of the depolarization rates allows qualitative conclusions regarding the strength of the electron-phonon coupling in the compounds under investigation. The dependence of the transition temperature on the condensate density of the halide-carbide superconductors is compared to that of other exotic superconductors.

I. INTRODUCTION

In the past decades, superconductors with layered crystal structures were intensively investigated, because they display a variety of unusual electronic properties. The most prominent examples are the high- T_c cuprate systems which exhibit exceptionally high transition temperatures at optimal doping. In the tantalum and niobium dichalcogenides and their intercalated derivatives a transition between quasi-two-dimensional and three-dimensional anisotropic superconductivity could be achieved by tuning the layer distances.^{1,2} Also the organic superconductors which exhibit a charge transfer from the separating layers to the conducting layers attracted much interest despite their modest transition temperatures.^{3,4}

While an explanation for the observed behavior in these systems based on a microscopic theory is still lacking, there appears to be general agreement that basically two effects dominate the electronic properties in these “exotic” materials: First, the layered crystal structures give rise to a pronounced anisotropy of their electronic properties. Band-structure calculations reveal bands with low dispersion (“flat bands”) which establish a structured electronic densities of states (DOS) at the Fermi level. When two flat bands cross with opposite curvature to form a saddle point at the Fermi surface the DOS diverges with a logarithmic curvature. The occurrence of such a “Van-Hove singularity” causes dramatic consequences on the electronic properties, e.g. deviations from Fermi-liquid behavior may be expected due to enhanced electron correlations.^{5,6} Second, in all of the “exotic” systems the charge carrier densities in the normal state are low. Therefore, charge screening which is effective in normal metals on a length scale of some Å is reduced and electron correlations become pronounced over an extended length scale. These effects also influence the order parameter in the superconducting state. If the coherence length $\xi_{\perp}(0)$ is much smaller than the layer spacing, the order parameter becomes quasi-two dimensional.² The subscripts \parallel and \perp in-

dicating an orientation parallel and perpendicular to the layers in the structure of the corresponding compounds, respectively. The amplitude of the order parameter is related to the superconducting charge carrier density n_s and the superconducting properties are assumed to be strongly affected by phase fluctuations if the superconducting charge carrier concentration is reduced below a certain limit.^{7,8} This statement was evidenced in the T_c vs $\sigma_{\text{FLL}}(0)$ plot by Uemura *et al.*,^{9,10} which shows a linear dependence of the transition temperature on the transverse-field muon spin relaxation (TF- μ SR) depolarization rates $\sigma_{\text{FLL}}(0) \propto n_s$ for many exotic superconductors.

In this contribution we present TF- μ SR investigations on the layered carbide halides $Y_2C_2X_2$, $X = \text{Br, I}$, and their three-dimensional relative YC_2 . The aim of our experiments was to evaluate the magnetic-field penetration depth λ which is one of the fundamental parameters of the superconducting state. In clean-limit superconductors $1/\lambda^2$ is proportional to the superconducting carrier density n_s divided by their effective mass m^* . For the determination of absolute values for the magnetic penetration depth and condensate densities TF- μ SR measurements provide a powerful tool.¹¹ The present investigations have been performed on polycrystalline powder samples of the superconductors YC_2 and the highly anisotropic $Y_2C_2X_2$ because no single crystals of suitable size and quality are available to our knowledge.

The crystal structures of the $Y_2C_2X_2$ compounds consist of closely packed yttrium metal atom bilayers which are sandwiched between sheets of halogen atoms (Fig. 1). Quasimolecular C_2 dumbbells occupy octahedral voids to form Y_6C_2 units condensed into layers which are surrounded by halogen atom layers. Such $X\text{-Y-C}_2\text{-Y-X}$ layered units stack and form a structure with monoclinic symmetry. A detailed discussion of the stacking sequences and lattice properties of the rare-earth carbide halides can be found in Ref.12. The layered compounds $Y_2C_2X_2$ are structurally related to the superconducting carbide YC_2 . The latter compound consists

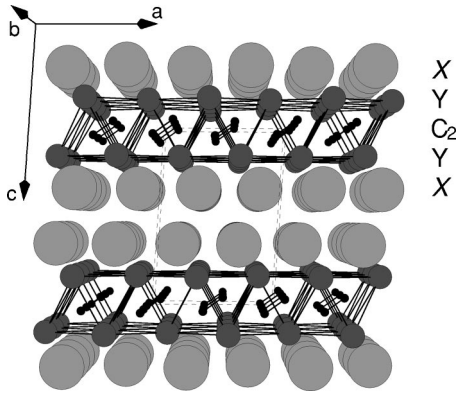


FIG. 1. Perspective projection of the crystal structure of $Y_2C_2X_2$ along [010]. Halogen atoms are represented by large circles and rare-earth metal atoms by smaller circles. The octahedral voids of the yttrium atom bilayers are occupied by C_2 units (small filled circles). The dashed lines indicate the monoclinic unit cell.

of a three-dimensional network of the same Y_6C_2 units.^{13,14}

Since the discovery of superconductivity in the rare-earth carbide halides $Y_2C_2X_2$, considerable work has been devoted to an understanding of their physical behavior in the superconducting state.^{15–26} Extensive investigations have revealed a variety of characteristic properties. For example, in the $Y_2C_2Br_{2-x}I_x$ series a pronounced peak in $T_c(x)$ was observed at a bromine to iodine ratio of 1:3 ($x = 1.5$), see Ref. 22. For $Y_2C_2Br_{0.5}I_{1.5}$ the transition temperature reaches 11.6 K, which is close to the T_c 's of the organic or Chevrel-phase superconductors. The superconducting states of the compounds $Y_2C_2Br_2$ ($T_c = 5.04$ K), $Y_2C_2I_2$ ($T_c = 9.97$ K), and YC_2 ($T_c = 4.05$ K) have been investigated in great detail by means of $C_p(T, B)$ and $M(T, B)$ experiments.^{14–19} These experiments reveal an enhanced electron-phonon coupling in the halide superconductors while YC_2 exhibits textbook-like BCS weak-coupling behavior. The layered compounds $Y_2C_2X_2$ were found to be high- κ superconductors ($\kappa \approx 60$ for $Y_2C_2I_2$) and have critical fields of $B_{c2} = 3 \pm 0.2$ T and $B_{c2} = 11.8 \pm 0.2$ T for the bromine and iodine compounds, respectively. For $Y_2C_2I_2$ an anisotropy ratio of the coherence length of $\gamma = \xi_{\parallel} / \xi_{\perp} = 5.2 \pm 0.2$ was derived from magnetic ac-susceptibility investigations on single crystals. The in-plane and out-of-plane coherence lengths of $\xi_{\parallel} = 133$ Å and $\xi_{\perp} = 26$ Å considerably exceed the lattice constants. Therefore, the superconducting order parameter of $Y_2C_2I_2$ is strongly anisotropic but still extends across several layer units. On the other hand, the Ginzburg-Landau parameter of the binary carbide YC_2 is close to the type-I limit ($\kappa_{GL} \approx 1$), and the critical field $B_{c2} = 60 \pm 10$ mT is much reduced compared to those of the carbide halides.^{14,17,28}

Band structure calculations with the tight-binding linear muffin-tin orbital TB-LMTO method indicate that an overlap of antibonding $C_2-\pi^*$ molecular orbitals with energetically neighboring $Y-d$ states is responsible for the metallic character of the $Y_2C_2X_2$, see Ref. 22. This covalence is evidenced by the short C-C bond distance of 128 ± 2 pm, Ref. 18. The band-structure calculations also reveal a pronounced peak in the electronic density of states close to the Fermi energy due to a saddle point at the Fermi surface in $Y_2C_2Br_2$. The Fermi energy falls in a region where the DOS decreases with a positive curvature with increasing energy. This find-

TABLE I. Lattice parameters of the present carbide superconductors.

Compound	a (pm)	b (pm)	c (pm)	β (deg)
$Y_2C_2Br_2$	695.4(1)	376.5(1)	993.1(1)	99.99(2)
$Y_2C_2Br_{0.5}I_{1.5}$	715.3(2)	385.2(1)	1038.4(2)	93.90(4)
$Y_2C_2I_2$	721.7(1)	288.3(1)	1043.7(1)	93.68(1)
$YC_{2-\delta}$	366.37(2)	366.37(2)	617.32(5)	90

ing is supported by ^{13}C -NMR experiments, which show deviations from a linear temperature dependence of the Korringa relaxation²⁵ and the pressure dependence of T_c in the $Y_2C_2X_2$ series.²⁶ The structure in the DOS has been discussed to be of significant importance for the superconducting state in the yttrium carbide halide materials.^{21–23}

II. SAMPLE PREPARATION AND CHARACTERIZATION

Single phase samples of $Y_2C_2X_2$ were synthesized by reacting stoichiometric amounts of yttrium metal chips (99.999% Johnson-Matthey), YOX free YX_3 salts and graphite powder (Aldrich Chemie). YX_3 was prepared as reported in Ref.27 and purified by sublimating YX_3 several times in high vacuum in an especially designed tantalum container. The ingredients were sealed in tantalum crucibles and reacted at 1300 K for several days. The reaction was terminated by quenching the samples to room temperature.²⁰ The precursor materials and the products are sensitive to air and moisture. Therefore, all procedures were carried out in a dried argon or helium gas atmosphere. The YC_2 sample was prepared by arc-heating of stoichiometric quantities of yttrium metal chips and graphite pieces (Deutsche Carbone 99.999%) in dried argon gas atmosphere. Subsequently, the pellets were sealed in tantalum crucibles and annealed at temperatures between 1200 and 2300 K for 10 days.

All samples under investigation were characterized by x-ray diffraction measurements to prove phase purity and to compare the crystallographic data with the literature^{12,20} (see Table I). dc magnetization measurements were performed to check the superconducting properties, e.g., the transition temperatures, magnetic shielding, and Meissner fraction.

The lattice parameters of the investigated yttrium carbide halide samples agree with the literature data within experimental error. No additional lines due to impurity phases were found. The diamagnetic shielding is complete in all yttrium carbide halide samples and the Meissner fraction typically reaches 30% of full magnetic shielding. The YC_2 sample used in the μ SR experiments exhibits a lower transition temperature $T_c = 3.85$ K as reported previously in Ref.14. Moreover, the c -lattice parameter of the investigated sample is reduced with respect to that which has been found in samples with a transition temperature of $T_c \approx 4.0$ K. A comprehensive analysis of the sample characteristics and the dependence on the preparation conditions has led to the conclusion that local carbon defects of about 2.5%/C are responsible for the observed reduction of T_c and the shortening of the c -lattice parameter in our sample.¹⁴ Therefore, the present yttrium dicarbide sample is assigned as $YC_{2-\delta}$ in the following, with $\delta \approx 0.05$. Relying on this fact we conclude that our

$\text{YC}_{2-\delta}$ sample is not in the clean limit which has to be taken into account for the interpretation of the TF- μ SR data in Sec. IV.

III. THE TF- μ SR EXPERIMENTS

A comprehensive discussion of the TF- μ SR technique is provided in Ref. 29, and the used instruments are described in detail in Ref. 30. Here, we give only a brief description of the method, which is necessary for an understanding of the data analysis. The TF- μ SR experiments above (below) $T = 2$ K were performed using a standard ^4He gas-flow cryostat (^3He dilution cryostat) at beamline πM3 , both at the Paul-Scherrer-Institut in Villigen, Switzerland. *In situ* pressed disc-shaped pellets of 10 mm diameter and about 2 mm thickness were sealed in especially designed sample holders made of high purity silver. The pellets were enclosed in dry helium gas behind a 100 μm Mylar window to avoid exposure to water and oxygen. The samples were fixed with small amounts of dried silicon grease to guarantee thermal contact to the environment. After cooling the sample in an external field of $B_{\text{ext}}=0.1$ T to temperatures below T_c in order to induce a homogeneous flux line lattice (FLL), positive muons with initial spin polarization $\vec{P}_\mu(t=0)$ transverse to the external field B_{ext} were implanted. The muons come to rest at interstitial lattice sites which are yet unknown for the present compounds. However, since the characteristic length λ of the FLL is significantly larger than the lattice parameters, the implanted muons are randomly distributed throughout the FLL field profile. Each muon spin starts to precess in its local field with the Larmor frequency $\omega_\mu = \gamma_\mu B_{\text{loc}}$ ($\gamma_\mu = 2\pi \cdot 135.5$ MHz/T). After an average lifetime of $\tau = 2.2$ μs the muons decay emitting positrons preferably into the direction of the muon spin $\vec{P}_\mu(t)$. The resulting asymmetric positron-emission rate $N_{e^+}(t)$ includes all the information on the precession frequencies and depolarization rates of $\vec{P}_\mu(t)$. The Fourier transform $F(\omega_\mu)$ of $N_{e^+}(t)$ yields the distribution of the precession frequencies of the muon spins and thus of the FLL field profiles. For polycrystalline samples typically almost symmetric Gaussian-shaped distributions $F(\omega_\mu)$ are detected (see inset of Fig. 2) for which the second moments $\langle \Delta\omega_\mu^2 \rangle$ may be extracted by fitting the TF- μ SR time spectra $P_\mu(t)$ by an exponential term $\exp(-\sigma_{\text{eff}}^2 t^2/2)$ (for the definition of σ_{eff} see Ref. 32) as is shown in Fig. 2. Here, the depolarization rate σ_{eff} of the initial muon-spin polarization $P_\mu(0)$ is proportional to the second moment of the frequency distribution $\sigma_{\text{eff}} \propto \langle \Delta\omega_\mu^2 \rangle$. The magnetic penetration depth of a polycrystalline type-II superconductor can be evaluated from the depolarization rate:

$$\begin{aligned} \sigma_{\text{FLL}}(T) \text{ (}\mu\text{s}^{-1}\text{)} &= \sqrt{\sigma_{\text{eff}}^2(T) - \sigma_{\text{nuc}}^2} \\ &= 1.072 \times 10^5 \lambda_{\text{poly}}^{-2}(T) \text{ (nm)}, \end{aligned} \quad (1)$$

wherein nuclear contributions σ_{nuc} to the effective muon depolarization have been subtracted.²⁹ In order to check the reliability of the λ values obtained from the time spectra $P_\mu(t)$ we additionally analyzed the Fourier transforms $F_\mu(\omega)$. Figure 2 displays the time spectrum of a data set recorded with the $\text{Y}_2\text{C}_2\text{I}_2$ sample at $T=3.0$ K in an external

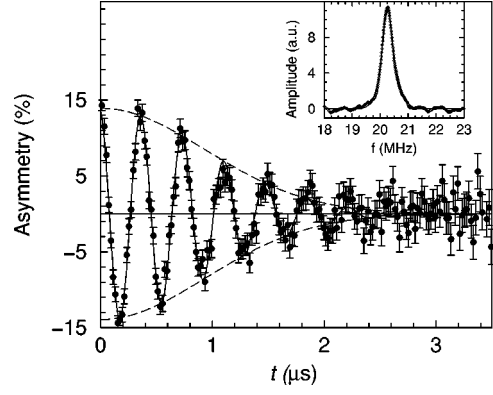


FIG. 2. Asymmetry versus time spectrum for $\text{Y}_2\text{C}_2\text{I}_2$ recorded at $T=3.0$ K in an external field of $B_{\text{ext}}=150$ mT displayed in a rotating reference frame. The full line displays the fit $A(t)=a\exp(-\sigma_{\text{eff}}^2 t^2)\cos(\omega t)$. The exponential decay of the asymmetry signal $P_\mu(t)=\exp(-\sigma_{\text{eff}}^2 t^2)$ includes the effective depolarization rate σ_{eff} . The inset contains the real part of the Fourier transform $F_\mu(\omega)$ of the time spectrum below. A fit of two Gaussian lines has been applied in order to account for a background signal arising from muons which stop in the silver backing of the sample holder ($\approx 3\%$ asymmetry).

field of $B_{\text{ext}}=150$ mT. The good agreement of Gaussians with the recorded time spectra is evidenced in the inset of Fig. 2.

In highly anisotropic superconductors, the flux lines are no longer in direction of the external field but are almost aligned parallel to the layers. Therefore, the second moment of the frequency distribution has a dominant contribution of the in-plane component of the magnetic penetration depth λ_{\parallel} , and the equation

$$\lambda_{\text{poly}} \approx 1.23 \times \lambda_{\parallel} \quad (2)$$

was shown to hold for $\gamma = \lambda_{\perp} / \lambda_{\parallel} > 5$, Ref. 31. The depolarization rate σ_{FLL} of the initial spin polarization measured on polycrystalline samples of a highly anisotropic type-II superconductor provides therefore a direct measure of the in-plane penetration depth λ_{\parallel} and hence of the ratio of the superconducting condensate density n_s to the effective mass m_{\parallel}^*

$$\begin{aligned} \sigma_{\text{FLL}}[\mu\text{s}^{-1}] &= 7.086 \times 10^4 \lambda_{\parallel}^{-2} \text{ (nm)} \\ &= 2.51 \times 10^{-21} \frac{m_e}{m_{\parallel}^*} n_s (\text{cm}^{-3}). \end{aligned} \quad (3)$$

It is known that a nearly symmetric and Gaussian line shape should be expected in polycrystalline samples due to random orientations of the grains of a superconductor with strongly anisotropic properties and the variation of the magnetization in the grains,³⁴ as it is in the present investigation (see Fig. 2). The influence of unusual flux states, pinning, and flux dynamics, however, cannot be directly gained (as they can in single-crystal materials), and these may induce systematic uncertainties in the second moments $\langle \Delta\omega_\mu^2 \rangle$ derived from μ SR data on polycrystalline samples. For example, the vortex-core radii and thus the field distributions of the vortices may be strongly field and temperature dependent as it is known for the layered superconductor NbSe_2 (see

Ref. 35). These systematic uncertainties have been the reason for objections to the interpretation of μ SR data on polycrystalline samples by means of a simple Gaussian analysis.³⁶ Therefore we emphasize that the quoted errors in $\lambda(0)$ only relate to the statistical errors of the Gaussian analysis, and do not consider model-dependent uncertainties.

However, a systematic error in the second moment of the field distribution $\langle \Delta B_{\text{loc}}^2 \rangle$ and $\sigma_{\text{eff}} \propto \langle \Delta \omega_{\mu}^2 \rangle$ of 25% due to the influence of pinning effects or unusual flux states, would induce a variation of only 7% in the resulting penetration depth values.²⁹ Thus, despite all shortcomings mentioned above, there is reasonable consistency between the $\sigma(0)$ and $\lambda_{\parallel}(0)$ values that have been derived from TF- μ SR experiments on polycrystalline or single-crystalline samples of some cuprate superconductors.^{29,33,37}

IV. RESULTS AND DISCUSSION

In all investigated carbide superconductors we observed one distinct temperature dependent TF- μ SR depolarization rate which clearly proves the existence of a FLL over the total sample volume.

In the following, the experimental results of the TF- μ SR investigations are discussed. First, the field dependences of the depolarization rates σ_{FLL} of $\text{YC}_{2-\delta}$ and $\text{Y}_2\text{C}_2\text{I}_2$ recorded at $T=2.1$ K are compared. From an analysis of $\sigma(T=2.1 \text{ K}, B_{\text{ext}})$ data a field regime is found for which the London limit holds and the evaluation of λ is reliable. The subsequent measurements of the temperature dependences of the depolarization rates have been performed within these field ranges. The $\lambda(T)$ data are compared to results of previous $C_p(T, B)$ investigations which reveal a strong electron-phonon coupling in the $\text{Y}_2\text{C}_2\text{X}_2$ systems. From an extrapolation $\sigma_{\text{FLL}}(T \rightarrow 0)$, the superconducting charge carrier densities are obtained. These results are discussed in the scheme of the T_c vs $\sigma_{\text{FLL}}(0)$ -plot which reveals a linear relation of T_c and $\sigma_{\text{FLL}}(T \rightarrow 0) \propto n_s/m_{\parallel}^*$ in the underdoped regime of the high- T_c cuprates and other exotic superconductors.¹⁰

A. The field dependence of the depolarization rate

Equation (2) has been shown to be only meaningful if the external magnetic field B_{ext} is within a range where the second moments of the field distribution $\langle \Delta B_{\mu}^2 \rangle \propto \langle \omega_{\mu}^2 \rangle \propto \sigma_{\text{eff}}$ are independent of the applied field B_{ext} , Refs. 11 and 33. The dependence of σ_{eff} on B_{ext} has been investigated in order to find a field range meeting the requirements of the London model. Figure 3 displays the field dependency σ_{eff} for samples of the $\text{YC}_{2-\delta}$ and $\text{Y}_2\text{C}_2\text{I}_2$ superconductors. Each data point has been obtained from a single time spectrum $P_{\mu}(t)$ which was recorded after cooling the sample in the applied field from temperatures above T_c to 2.1 K. Both $\sigma_{\text{eff}}(T=2.1 \text{ K}, B_{\text{ext}})$ curves exhibit a cusp in the low-field range. For the $\text{Y}_2\text{C}_2\text{I}_2$ sample, $\sigma_{\text{eff}}(T=2.1 \text{ K}, B_{\text{ext}})$ increases until reaching a maximum value of $1.17 \mu\text{s}^{-1}$ at $B_{\text{ext}} \approx 30$ mT. Above $B_{\text{ext}} \approx 80$ mT the effective depolarization becomes independent of the applied field. The situation for the $\text{YC}_{2-\delta}$ superconductor is more complicated because this compound is very close to the type-I type-II transition^{38,14} ($\kappa_{\text{GL}} \approx 1$) where nonmagnetic impurities and defects quanti-

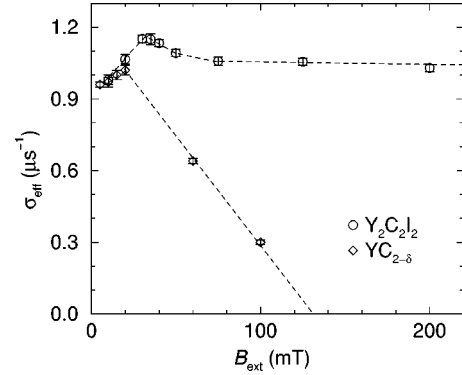


FIG. 3. Dependence of the depolarization rate $\sigma_{\text{eff}}(T=2.1 \text{ K})$ on the applied magnetic field for $\text{Y}_2\text{C}_2\text{I}_2$ (circles) and $\text{YC}_{2-\delta}$ (diamonds). The dashed lines were drawn to guide the eye. For $\text{Y}_2\text{C}_2\text{I}_2$ the depolarization is nearly constant for external fields above 80 mT. In the case of $\text{YC}_{2-\delta}$ no field regime satisfies the requirements of the London limit. The critical field $B_{c2} \approx 130$ mT of the investigated $\text{YC}_{2-\delta}$ sample is higher than that of a clean-limit sample (see text).

tatively affect the magnetic phenomena in the superconducting state. In the dirty limit ($l \ll \xi$) the reduction of the normal-state mean free path l due to defects reduces the coherence length in the superconducting state $\xi_{\text{eff}} \propto \sqrt{\xi_{\text{clean}} \cdot l}$ and increases the critical field $H_{c2} \propto 1/\xi_{\text{eff}}^2$, Ref. 39. The crystallographic characterization of our sample reveals a reduced c -lattice parameter (see Table I) indicating a carbon deficiency. Also the reduced T_c and the higher critical field $B_{c2}(T=2.1 \text{ K}) \approx 130$ mT as compared to the results from the clean limit sample^{14,38} give further evidence for the investigated yttrium dicarbide sample to be in the dirty limit (Fig. 3). According to the $\sigma_{\text{eff}}(B_{\text{ext}})$ dependence, the applied field for the determination of the London penetration depth $\lambda(0)$ for $\text{Y}_2\text{C}_2\text{X}_2$ must be larger than 80 mT, while for $\text{YC}_{2-\delta}$ a reliable evaluation of $\lambda(0)$ from Eq. (3) is not meaningful.

The low-field cusp in $\sigma_{\text{eff}}(B)$ was observed before for polycrystalline high- T_c superconductors.²⁹ The cusp was explained⁴⁰ as due to a pinning-induced distortion of the flux line lattice, which enhances $\langle \Delta B_{\mu}^2 \rangle$ and results in a higher value for the depolarization σ_{eff} . The observation of such a cusp at low magnetic fields implies that pinning effects are weak and negligible at higher fields. This indicates the absence of strong pinning centers, e.g. lattice distortions or impurity phases, and evidences the high-quality and structural homogeneity of the investigated $\text{Y}_2\text{C}_2\text{I}_2$ sample.²⁹

B. The temperature dependence of the depolarization rate

In order to evaluate the London penetration depth from the TF- μ SR depolarization rates σ_{eff} , the nuclear contributions σ_{nuc} were subtracted according to Eq. (1). Above T_c , the internal field distribution is not affected by the FLL and a temperature-independent μ SR depolarization occurs due to the magnetic field induced by nuclear moments. For $\text{Y}_2\text{C}_2\text{I}_2$ and $\text{YC}_{2-\delta}$ the temperature dependence of $\sigma_{\text{FLL}}(t)/\sigma_{\text{FLL}}(0)$ is compared to the theoretical function of BCS theory

$$\frac{\sigma_{\text{FLL}}(t)}{\sigma_{\text{FLL}}(0)} = \frac{1}{1 - \frac{\partial \ln \Delta(t)}{\partial \ln t}}, \quad (4)$$

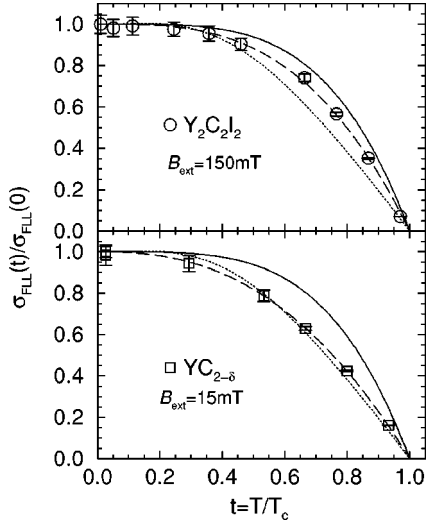


FIG. 4. Temperature dependence of the normalized effective muon depolarization rate taken at 150 and 15 mT for $Y_2C_2I_2$ and $YC_{2-\delta}$, respectively. For $Y_2C_2I_2$ (open circles) and $YC_{2-\delta}$ (open squares) data were fitted to a power law $1-t^n$ (dashed lines) with $n=3.1$ and 2.5 , respectively. Data are compared to BCS weak coupling (dotted line) and 2FL model (full line) assuming a $\sigma_{FLL} \propto 1/\lambda_{poly}^2$ relation.

where $\Delta(t)$ is the temperature dependence of the BCS-gap width⁴¹ and $t=T/T_c$. Additionally, a power law

$$\frac{\sigma_{FLL}(t)}{\sigma_{FLL}(0)} = 1 - t^n \quad (5)$$

has also been fitted to the data, where $n=4$ corresponds to the two-fluid (2FL) model.⁴²

The $\sigma_{FLL}(t)/\sigma_{FLL}(0)$ data are in qualitative agreement with the investigations of the specific-heat jump at T_c . In the case of $YC_{2-\delta}$, the data pass along the theoretical curve of the BCS model for weak electron-phonon coupling, and are fitted by a power law with a power of $n=2.5$. However, we note that there is no applied magnetic field to hold the London limit for $YC_{2-\delta}$ [and thus there is no simple relation between σ_{FLL} and the London penetration depth as in Eq. (1)]. Nevertheless, the observed $\sigma_{FLL}(t)/\sigma_{FLL}(0)$ data are in fair agreement with BCS theory assuming a $\sigma_{FLL} \propto 1/\lambda_{poly}^2$ relation (see Fig. 4).

For $Y_2C_2I_2$, the power-law fit results in an exponent of $n=3.1$, which is significantly enhanced with respect to that of $YC_{2-\delta}$. Here, $\sigma_{FLL}(t)/\sigma_{FLL}(0)$ data have larger values than according to BCS theory and are shifted in the direction of the 2FL model. The large value of the exponent $n=3.1$ qualitatively indicates an enhanced electron-phonon coupling in $Y_2C_2I_2$. The analysis of $\sigma_{FLL}(t)/\sigma_{FLL}(0)$ supports the the heat-capacity data for both samples: According to the analysis of the specific-heat jump at T_c using the α model,⁴³ the gap width of YC_2 amounts to a value of $\alpha=\Delta(0)/k_B T_c=1.82$, which is close to the BCS value of $\alpha=1.79$ and indicates weak electron-phonon coupling for this compound.¹⁷ On the other hand, a significantly increased gap width of $\alpha=\Delta(0)/k_B T_c=2.27$ has been reported for $Y_2C_2I_2$, which implies strong electron-phonon coupling. In the context with the above results it should be mentioned that there is a marked disagreement of the $\sigma_{FLL}(t)/\sigma_{FLL}(0)$ depen-

TABLE II. Critical temperatures T_c , depolarization rate $\sigma_{FLL}(0)$, and absolute values for the London penetration depth $\lambda_{poly}(T \rightarrow 0)$ which was calculated using Eq. (1).

Compound	T_c (K)	$\sigma_{FLL}(0)$ (μs^{-1})	$\lambda_{poly}(0)$ (nm)
$Y_2C_2Br_2$	5.05	0.35 ± 0.02	553 ± 5
$Y_2C_2Br_{0.5}I_{1.5}$	11.6	0.22 ± 0.07	698 ± 10
$Y_2C_2I_2$	9.97	1.07 ± 0.02	317 ± 3
$YC_{2-\delta}$	3.85	1.25 ± 0.03	(810 ± 50) Ref. 46

dence between polycrystalline samples and single crystals of high- T_c cuprates, which has not yet been understood.^{29,44} The above results support s-wave symmetry of the superconducting order parameter in all investigated compounds. Final conclusive evidence on the nature of the order parameter, however, can only be gained from investigations on single crystals.

C. The London penetration depth

The London penetration depths $\lambda(0)$ of the $Y_2C_2X_2$ compounds have been evaluated in the scope of London theory by extrapolating the low-temperature TF- μ SR depolarization $\sigma_{FLL}(T \rightarrow 0)$. The values of the London penetration depths, which were taken from polycrystalline samples have been deduced according to Eq. (1) and are compiled in Table II. In the case of $YC_{2-\delta}$, the evaluation of the magnetic penetration depth is not meaningful because there is no field range where the London limit applies (see Chap. IV A). The $\lambda(0)$ values gained from the present μ SR experiments are in excellent agreement with those which were reported from an analysis of the magnetization data for the same $Y_2C_2X_2$ compounds.¹⁷ However, the accuracy of the present $\lambda(0)$ values is about one order of magnitude higher (the estimated error about one order of magnitude lower) as for the magnetization measurements reported in Ref.17.

Investigations of the upper critical field of a $Y_2C_2I_2$ crystal yield an anisotropy ratio of $\gamma = \xi_{||} / \xi_{\perp} = 5.2 \pm 0.2$. This value is similar to that reported for fully oxygenated (slightly overdoped) $YBa_2Cu_3O_{7-x}$, Ref. 45, and Eq. (2) may be used in the case of $Y_2C_2I_2$ in order to obtain the in-plane component of the London penetration depths $\lambda_{||} = 257 \pm 3$ nm. With $\gamma \approx 5.2$, the out-of-plane value of the penetration depth of $Y_2C_2I_2$ amounts to $\lambda_{\perp} = 1340 \pm 50$ nm.

D. The superconducting charge carrier density

The shielding currents of a superconductor penetrate in the length scale of the magnetic penetration depth $\lambda(0)$ which is directly related to the superconducting condensate density $n_s(0)/m^*$ for clean limit superconductors [see Eq. (3)]. Uemura *et al.* were the first to realize that the transition temperatures of the underdoped cuprates when plotted versus the TF- μ SR depolarization rate $\sigma_{FLL}(T \rightarrow 0) \propto n_s(0)/m^*$ fall on a common line.¹⁰ An explanation for this amazing finding was proposed by Emery *et al.*⁸ who suggested that phase fluctuations of the order parameter in the superconducting state become increasingly pronounced with decreasing con-

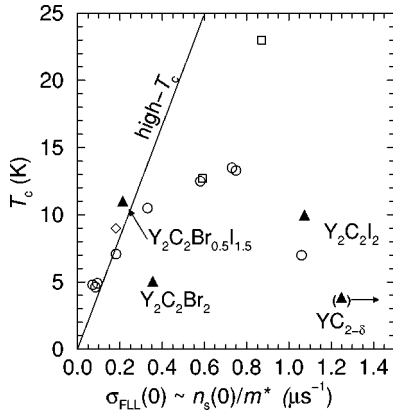


FIG. 5. Superconducting transition temperature versus $\sigma_{\text{FLL}}(T \rightarrow 0)$. The yttrium carbide superconductors are compared to other exotic systems. The open symbols refer to results on BEDT, $(\text{Ba}_x\text{K}_{1-x})\text{BiO}_3$, and Chevrel superconductors (diamonds, squares, and circles, respectively; data were taken from Ref. 10). The full triangles present data for $\text{Y}_2\text{C}_2\text{Br}_2$, $\text{Y}_2\text{C}_2\text{I}_2$, $\text{Y}_2\text{C}_2\text{Br}_{0.5}\text{I}_{1.5}$, and $\text{YC}_{2-\delta}$. In the case of $\text{YC}_{2-\delta}$ the relation $\sigma_{\text{FLL}}(T \rightarrow 0) \propto n_s(0)/m^*$ is not valid and data for $\text{YC}_{2-\delta}$ must be regarded as a lower limit for $n_s(0)/m^*$.

condensate densities $n_s(0)$ and suppress the superconducting transition temperatures according to $T_c \propto n_s(0)/m^* \propto \sigma_{\text{FLL}}(T \rightarrow 0)$.

It was shown later that other unconventional superconductors also lie close to the Uemura line.¹⁰ Figure 5 displays the low- T_c low $\sigma_{\text{FLL}}(0)$ regime of the T_c vs $\sigma_{\text{FLL}}(0)$ plot. Full triangles reflect the values for the present carbide superconductors. While $\text{Y}_2\text{C}_2\text{Br}_2$ and $\text{Y}_2\text{C}_2\text{Br}_{0.5}\text{I}_{1.5}$ are located close to the Uemura line, $\text{Y}_2\text{C}_2\text{I}_2$ deviates like the optimal and overdoped high- T_c superconductors.

The depolarization rate $\sigma_{\text{FLL}}(T \rightarrow 0)$ and thus the superconducting condensate density of $\text{Y}_2\text{C}_2\text{Br}_{0.5}\text{I}_{1.5}$ is somewhat reduced with respect to that of $\text{Y}_2\text{C}_2\text{Br}_2$. For the mixed halogen compound $\text{Y}_2\text{C}_2\text{Br}_{0.5}\text{I}_{1.5}$, the different halogen atoms are randomly distributed throughout the halogen sites, which results in a distribution of the crystal potentials and may give rise to localization effects. This may reduce the charge carrier density in the normal state and also the condensate density in the superconducting state and shifts the μSR depolarization $\sigma_{\text{FLL}}(T \rightarrow 0)$ to lower values than for the corresponding compound without localization. Experimental evidence for localization effects in the mixed halogen compound $\text{Y}_2\text{C}_2\text{Br}_{2-x}\text{I}_x$ were gained from investigations of the temperature dependence of the electrical resistance.¹⁷ Also $\sigma_{\text{FLL}}(T \rightarrow 0)$ for the investigated $\text{YC}_{2-\delta}$ sample is much smaller than for other weak-coupling BCS superconductors because the charge carrier density is likely limited by electron localization due to a reduction of the carbon content. Therefore, the $\sigma_{\text{FLL}}(T \rightarrow 0)$ data for $\text{YC}_{2-\delta}$ which is inserted in Fig. 5 must be regarded as a lower limit with respect to values expected for a clean limit YC_2 sample.

In the T_c vs $\sigma_{\text{FLL}}(0)$ plot the investigated carbide superconductors are located in the vicinity to Chevrel phases, organic BEDT, and $\text{Ba}_x\text{K}_{1-x}\text{BiO}_3$ superconductors. The different values for the depolarization rates $\sigma_{\text{FLL}}(T \rightarrow 0)$ in the $\text{Y}_2\text{C}_2\text{Br}_{2-x}\text{I}_x$ series can be explained by a systematic change in $N(\epsilon_F)$: Recent investigations of the pressure dependences of T_c in the $\text{Y}_2\text{C}_2\text{Br}_{2-x}\text{I}_x$ series support a rigid-band model where the Fermi energy shifts through a peak in the DOS by increasing the iodine content x , see Ref. 26. The electronic specific-heat contribution nearly doubles for $\text{Y}_2\text{C}_2\text{I}_2$ with respect to $\text{Y}_2\text{C}_2\text{Br}_2$. This changes the charge carrier densities in the normal state and thus the condensate densities in the superconducting state in the $\text{Y}_2\text{C}_2\text{Br}_{2-x}\text{I}_x$ series and causes the observed increase of $\sigma_{\text{FLL}}(T \rightarrow 0)$.

V. SUMMARY

For all investigated carbide superconductors the recorded μSR spectra are well described by a single component relaxation function, proving the existence of a FLL over the entire sample volume. The investigations of the field and temperature dependences of the depolarization rates taken from $\text{Y}_2\text{C}_2\text{I}_2$ indicate weak pinning and high- κ superconductivity in agreement with results from magnetization data. For $\text{YC}_{2-\delta}$ which according to the reduced c -lattice parameter (Table I) exhibits a carbon deficiency, no field regime satisfies the requirements of the London model.

The temperature dependences $\sigma_{\text{FLL}}(t)/\sigma_{\text{FLL}}(0)$ support the results of the specific-heat investigations, namely, that YC_2 exhibits a weak electron-phonon coupling while it is enhanced in $\text{Y}_2\text{C}_2\text{I}_2$. The low temperature values of the μSR depolarization have been used to calculate the London penetration depth for the $\text{Y}_2\text{C}_2\text{X}_2$ superconductors. Moreover, in the case of $\text{Y}_2\text{C}_2\text{I}_2$ the in-plane and out-of-plane values of the London penetration depth were derived in context with the anisotropy ratio of the upper critical field.

In the T_c vs $\sigma_{\text{FLL}}(0)$ plot, the carbide materials lie close to the Chevrel phases, organic BEDT, and $\text{Ba}_x\text{K}_{1-x}\text{BiO}_3$ superconductors. $\text{Y}_2\text{C}_2\text{Br}_2$ and $\text{Y}_2\text{C}_2\text{Br}_{0.5}\text{I}_{1.5}$ are located close to the Uemura line. For these compounds, phase fluctuations of the superconducting order parameter were considered to limit the superconducting transition temperatures. For $\text{Y}_2\text{C}_2\text{Br}_{0.5}\text{I}_{1.5}$ and $\text{YC}_{2-\delta}$, defects and crystal inhomogeneities reduce the normal-state charge carrier densities and thus the superconducting condensate densities, which limits the observed $\sigma_{\text{FLL}}(T \rightarrow 0)$ values.

ACKNOWLEDGMENTS

We are very grateful to A. Amato, Ch. Baines, and D. Herlach (PSI) for their kind assistance during the μSR experiments. We are also very grateful to Hj. Mattausch and R. Eger for valuable discussions regarding the sample preparation.

- ¹F.R. Gamble, F.J. DiSalvo, R.A. Klein, and T.H. Geballe, *Science* **168**, 568 (1970).
- ²L.N. Bulaevskii, *Usp. Fiz. Nauk.* **115–117**, 449 (1975) [*Sov. Phys. Usp.* **18**, 514 (1975)].
- ³M. Dressel, O. Klein, G. Grüner, K.D. Carlson, H.H. Wang, and J.M. Williams, *Phys. Rev. B* **50**, 13 603 (1994).
- ⁴S. Wanka, D. Beckmann, J. Wosnitza, E. Balthes, D. Schweitzer, W. Strunz, and H.J. Keller, *Phys. Rev. B* **50**, 13 603 (1994).
- ⁵D.M. Newens, P.C. Pattnaik, and C.C. Tsuei, *Phys. Rev. B* **43**, 3075 (1990).
- ⁶C.C. Tsuei, *Physica A* **168**, 238 (1990).
- ⁷V.J. Emery, *Nature (London)* **337**, 306 (1989).
- ⁸V.J. Emery, and S.A. Kivelson, *Phys. Rev. Lett.* **74**, 3253 (1995).
- ⁹Y.J. Uemura, G.M. Luke, B.J. Sternlieb, J.H. Brewer, J.F. Carolan, W.N. Hardy, R. Kadono, J.R. Kempton, R.F. Kiefl, S.R. Kreitzman, P. Mulhern, R.M. Riseman, D.L. Williams, B.X. Yang, S. Uchida, H. Takagi, J. Gopalakrishnan, A.W. Sleight, M.A. Subramanian, C.L. Chien, M.Z. Cieplak, Gang Xiao, V.Y. Lee, B.W. Statt, C.E. Stronach, W.J. Kossler, and X.H. Yu, *Phys. Rev. Lett.* **62**, 2317 (1989).
- ¹⁰Y.J. Uemura, L.P. Le, G.M. Luke, B.J. Sternlieb, W.D. Wu, J.H. Brewer, R.M. Riseman, C.C. Seaman, M.B. Maple, M. Ishikawa, D.G. Hinks, J.D. Jorgensen, G. Saito, and H. Yamochi, *Phys. Rev. Lett.* **66**, 2665 (1991).
- ¹¹E.H. Brandt, *Phys. Rev. B* **37**, 2349 (1988).
- ¹²Hj. Mattausch, R.K. Kremer, R. Eger, and A. Simon, *Z. Anorg. Allg. Chem.* **609**, 7 (1992).
- ¹³M. Atoji, *J. Chem. Phys.* **35/6**, 1950 (1961).
- ¹⁴Th. Gulden, R.W. Henn, O. Jepsen, R.K. Kremer, W. Schnelle, A. Simon, and C. Felser, *Phys. Rev. B* **56**, 9021 (1997).
- ¹⁵R.W. Henn, W. Schnelle, R.K. Kremer, and A. Simon, *Phys. Rev. Lett.* **77**, 374 (1996).
- ¹⁶R.W. Henn, W. Schnelle, R.K. Kremer, and A. Simon, *Czech. J. Phys.* **46-S4**, 865 (1996).
- ¹⁷R.W. Henn, Ph.D. thesis, Universität Karlsruhe (TH), 1996.
- ¹⁸R.W. Henn, T. Strach, R.K. Kremer, and A. Simon, *Phys. Rev. B* **58**, 14 364 (1998).
- ¹⁹W. Schnelle, R.W. Henn, Th. Gulden, R.K. Kremer, and A. Simon, *J. Appl. Phys.* **83**, 7321 (1998).
- ²⁰U. Schwanitz-Schüller and A. Simon, *Z. Naturforsch. B* **40b**, 710 (1985).
- ²¹A. Simon, Hj. Mattausch, R. Eger, and R.K. Kremer, *Angew. Chem. Int. Ed. Engl.* **30**, 1188 (1991).
- ²²A. Simon, A. Yoshiasa, M. Bäcker, R.W. Henn, C. Felser, R.K. Kremer, and Hj. Mattausch, *Z. Anorg. Allg. Chem.* **622**, 123 (1996).
- ²³A. Simon, *Angew. Chem.* **109**, 4001 (1997).
- ²⁴M. Bäcker, Ph.D. thesis, Universität Stuttgart, 1997.
- ²⁵E. Herrling, E. Dormann, R.W. Henn, R.K. Kremer, and A. Simon, *Synth. Met.* **92**, 13 (1998).
- ²⁶R.W. Henn, K. Ahn, H.-A. Krug von Nidda, R.K. Kremer, and A. Simon, *Physica C* (to be published).
- ²⁷M.D. Taylor, *J. Inorg. Nucl. Chem.* **24**, 387 (1962).
- ²⁸Th. Gulden, Ph.D. thesis, Universität Stuttgart, 1997.
- ²⁹B. Pümpin, H. Keller, W. Kündig, W. Odermatt, I.M. Savic, J.W. Schneider, E. Kaldis, S. Rusiecki, Y. Maeno, and C. Rossel, *Phys. Rev. B* **42**, 8019 (1990).
- ³⁰PSI homepage <http://WWW1.psi.ch/herlach/instrum.html>.
- ³¹W. Barford and J.M.F. Gunn, *Physica C* **156**, 515 (1988).
- ³² σ_{eff} differs by a factor of 2 in the denominator of the exponent with respect to definitions given by other groups. This changes the factors in Eqs. (1) and (3) by a normalization factor of $\sqrt{2}$.
- ³³T.M. Riseman, J.H. Brewer, K.H. Chow, W.N. Hardy, R.K. Kiefl, S.R. Kreitzman, R. Liang, A. MacFarlane, P. Mendels, G.D. Morris, J. Rammer, and J.W. Schneider, *Hyperfine Interact.* **86**, 481 (1994).
- ³⁴A.J. Greer, W.J. Kossler, and K.G. Petzinger, *Hyperfine Interact.* **86**, 531 (1994).
- ³⁵J.E. Sonier, R.F. Kiefl, J.H. Brewer, J. Chakhalian, S.R. Dunsiger, A. MacFarlane, R.I. Miller, A. Wong, G.M. Luke, and J.W. Brill, *Phys. Rev. Lett.* **79**, 1742 (1997).
- ³⁶D.R. Harshman and A.T. Fiory, *Phys. Rev. Lett.* **72**, 2501 (1994), and references therein.
- ³⁷C. Bernhard, Ch. Niedermayer, U. Binniger, A. Hofer, Ch. Wenger, J.L. Tallon, G.V.M. Williams, E.J. Ansaldo, J.I. Budnick, C.E. Stronach, D.R. Noakes, and M.A. Blankson-Mills, *Phys. Rev. B* **52**, 10 488 (1995).
- ³⁸R.W. Henn, T. Gulden, W. Schnelle, R.K. Kremer, and A. Simon, *Czech. J. Phys.* **46-S2**, 641 (1996).
- ³⁹P.G. De Gennes and P.A. Pincus (Trans.), in *Superconductivity of Metals and Alloys*, edited by D. Pines (Benjamin, New York, 1966), p. 215ff.
- ⁴⁰R.F. Kiefl, T.M. Riseman, G. Aeppli, E.J. Ansaldo, J.F. Carolan, R.J. Cava, W.N. Hardy, D.R. Harshman, N. Kaplan, J.R. Kempton, S.R. Kreitzman, G.M. Luke, B.X. Jang, and D.L. Williams, *Physica C* **153-155**, 757 (1988).
- ⁴¹B. Mühlischlegel, *Z. Phys.* **155**, 313 (1959).
- ⁴²C.J. Gorter and H.B.G. Casimir, *Phys. Z.* **35**, 963 (1934).
- ⁴³H. Padamsee, J.E. Neighbor, and C.A. Shifman, *J. Low Temp. Phys.* **12**, 387 (1973).
- ⁴⁴J.E. Sonier, R.F. Kiefl, J.H. Brewer, D.A. Bonn, J.F. Carolan, K.H. Chow, P. Dosanjh, W.N. Hardy, R.X. Liang, W.A. MacFarlane, P. Mendels, G.D. Morris, R.M. Riseman, and J.W. Schneider, *Phys. Rev. Lett.* **72**, 744 (1994).
- ⁴⁵W. Bauhofer, W. Biberacher, B. Gegenheimer, W. Joss, R.K. Kremer, Hj. Mattausch, A. Müller, and A. Simon, *Phys. Rev. Lett.* **63**, 2520 (1989).
- ⁴⁶According to magnetization data, taken from Ref. 17.